Proc. SRI93 Conf. Synchr. Rad. (Gaithersburg, MD, 1993) August 17, 1993 1/8

Intensity Interferometry at the X13A Undulator Beamline

E. GLUSKIN, I. MCNULTY, L. YANG, and K.J. RANDALL
Advanced Photon Source, Argonne National Laboratory, Argonne, IL 60439, USA

E.D. JOHNSON
National Synchrotron Light Source, Brookhaven National Laboratory, Upton, NY 11973, USA

Abstract

We are constructing a soft x-ray intensity interferometer and an undulator based beamline to demonstrate intensity interferometry in the x-ray region. The 10-period soft x-ray undulator at the NSLS provides the necessary coherent flux; the X13A beamline is designed to preserve the spatial coherence of the bright x-ray beam and provide sufficient temporal coherence using a horizontally deflecting spherical grating monochromator. Using the interferometer, which consists of an array of small slits, a wedge-shaped beamsplitter and two fast microchannel plate detectors, we expect to measure the spatial coherence of the undulator beam and therefore the size of the source in the vertical plane. Details of the beamline design and the interferometer experiment are discussed.

1. Introduction

The 7-GeV Advanced Photon Source (APS) synchrotron radiation facility currently under construction will provide extremely bright (~10^{18} photons / (s mm^2 mrad^2 0.1% BW)), partially coherent x-rays in the intermediate and high energy regions [1]. However, an effective tool has yet to be developed to measure the degree of coherence of the radiation that does not require wavelength-scale alignment precision and stability. Determination of the coherence properties of synchrotron radiation sources is vital for coherence dependent applications such as x-ray microfocusing, holography and speckle methods, and in addition, can serve as an important diagnostic for characterization of the particle beam size and shape.

A conceptually elegant and potentially simple way of measuring the spatial coherence and source size of a synchrotron radiation beam is by intensity interferometry [2]. This technique was first demonstrated with visible light by Hanbury Brown and Twiss in 1956 using a mercury arc lamp as a source, then later used to measure the angular sizes of stars [3]. Unlike conventional

(amplitude) interferometers and related methods which rely on the phase difference between two or more interfering beams to form an interference pattern [4,5], an intensity interferometer measures the correlation between the intensity fluctuations of the two beams electronically. The chief advantage of the intensity interferometer is that because it responds only to fluctuations in the beam intensities, it is insensitive to phase variations in the beams caused by optical imperfections and path-length mismatch [6].

An intensity interferometer measures the modulus of the complex degree of coherence $|\mu_{12}|$ of the incident beam (equivalent to the fringe visibility that would be obtained with an amplitude interferometer) by electronically correlating the intensity fluctuations (or their time average) at two spatially separated points. The source size is obtained from $|\mu_{12}|$ by applying the Van Cittert-Zernike theorem [7], which in one dimension is given for a source intensity distribution s(y), wavenumber $k = 2\pi/\lambda$ and distance z from the source by

$$|\mu_{12}| = \left| \frac{\int s(y) e^{-iky\xi/z} dy}{\int s(y) dy} \right| \quad . \tag{1}$$

If the source is symmetrically disposed about the y-axis, s(y) can be obtained by inverse Fourier transformation of $|\mu_{12}|$.

The figure of merit for the feasibility of an intensity interferometry experiment is the source degeneracy parameter

$$\delta = B\frac{\lambda^3}{4c} \quad , \tag{2}$$

the number of photons per spatially and temporally coherent mode [6]. The degeneracy describes the likelihood for photons in the beam to bunch together in time. It is worthwhile to note that intensity interferometry is possible even when $\delta << 1$ as in the case of thermal-like sources, such as undulators, provided that the time resolution of the interferometer is sufficiently short and the measurement time is sufficiently long to obtain a statistically significant correlation. Fig. 1 shows the calculated δ for various synchrotron based x-ray sources.

The electron (or positron) beams in second and third generation storage rings are distributed in a larger extent in horizontal (x) than vertical (y) direction, resulting in an effective photon source that is considerably wider than it is tall. Due to the separability of the wave equation in orthogonal coordinates, it is possible to measure a much larger correlation signal with a one-dimensional measurement of the beam produced by such a source as compared to a two-

dimensional measurement. This can be accomplished by using slits instead of circular apertures, provided that the source size, slit sizes and slit spacing follow the same rules that would allow one to see fringes in a Young's double slit experiment with a line-shaped source [7]. The correlation signal thus obtained would be equivalent to a sum of the signals from many simultaneous pairs of points across the two slits. This effect can be exploited to dramatically reduce the time required for the coherence measurement.

In addition, it should be possible to take advantage of the pulsed time structure of the synchrotron radiation to decrease the measurement time. The duty cycle of many storage rings is typically less than 2% when operated in single bunch mode, which suggests that, at a minimum, the signal-to-noise ratio of the interferometer can be improved in proportion to the duty ratio by gating off sources of electronic noise between pulses of the radiation.

We plan to demonstrate intensity interferometry in the soft x-ray region with an experimental x-ray intensity interferometer mounted on the X13A undulator beamline at the National Synchtrotron Light Source (NSLS). The coherence measurement will be made in the vertical plane. In this paper we discuss the interferometer, the source, and the X13A beamline, which will also be used for other coherence dependent soft x-ray experiments.

2. Source characteristics

The X13 10-period soft x-ray "mini-undulator" was developed as a prototype for the 35-period X1 device installed elsewhere in the NSLS X-ray Ring [8]. Its magnetic structure is of the hybrid Halbach type with $SmCo_5$ magnetic material, steel poles, and an 8.0 cm period. The undulator gap can be adjusted from 32 to 90 mm, corresponding to a magnetic deflection parameter K of 0.17 to 2.3. At the storage ring energy of 2.5 GeV, the fundamental wavelength can be tuned from 1-6 nm with this range in K-values. Despite its short (1 m) length, the average brightness of this device in the soft x-ray region is substantial, about 10^{17} photons / (s mm^2 mrad^2 0.1% BW) at its optimum fundamental output wavelength of 3 nm. Based on the calculated degeneracy parameter for the X1 undulator (fig. 1), we estimate that a measurement of the spatial coherence of the beam can be obtained at X13 in several minutes.

The phase space of the source is dominated in the horizontal plane by that of the electron beam in the storage ring, thus little of the total flux is spatially coherent in this plane. In the vertical by contrast, approximately one third of the flux can contribute to the correlation measurement. The full-width at half-maximum (FWHM) source size and divergence are 920 μm, 590 μrad in the horizontal plane, and 47 μm, and 162 μrad in the vertical plane.

3. X13A beamline design

The X13A beamline is designed to provide moderate spectral resolution at 1-4 nm

wavelengths while preserving the coherence of the x-ray wavefront in the vertical dimension (see fig. 2). All beam deflections are made in the horizontal plane such as is done at the X1A beamline, whereas the diffraction grating has the same radius of curvature as that used at X1B.

A plane nickel-coated glidcop mirror, located 18.9 m from the source, deflects the x-ray beam by 4° to the X13A branchline. Two other beamlines, X13B (used for white-beam experiments) and X13C (used for 2-4 KeV experiments), currently exist adjacent to X13A and share the same mirror, which is rotated to direct the x-ray beam to the active beamline.

X13A employs a horizontally dispersing spherical grating monochromator (SGM) with a water cooled entrance slit (McPherson Corp.). The entrance slit aperture is adjustable from 5 μm to 1.2 mm and is fixed at 16.3 m from the source. The grating (Jobin-Yvon), located 2 m away at 18.3 m from the source, is nickel-coated and made of fused silica, has a groove density of 1200 lines/mm, 7-nm deep grooves, and a radius of curvature of 57.3 m. Its surface figure error is less than 2 μrad RMS and surface roughness is better than 0.4 nm. The included angle of the SGM is 173.5°, which centers the tuning range in the 1-4 nm wavelength band. The grating images the entrance slit onto the primary exit slit located at 4.6 m from the grating. The calculated resolving power of the SGM is shown in fig. 3. The peak resolving power is ~10^4 at the center wavelength of $\lambda = 2.3$ nm using 10 μm entrance and exit slit settings.

The entrance slit does not accept more than a small fraction of the undulator beam using the plane mirror. For experiments requiring spatial coherence in two dimensions this does not affect the coherent flux, however we wish to use the full horizontal swath of the beam in the intensity interferometry experiment. To do so, the entrance slit is opened up and the undulator source itself is sagitally focused onto an auxiliary exit slit located at 4.1 m from the grating. This entrance-slitless, fixed exit slit geometry has a narrow tuning range due to defocus aberration, nevertheless it provides adequate energy resolution for the experiment and avoids the complexity and expense of a movable slit. In the future we hope to install a cylindrical mirror to focus the beam sagitally onto the entrance slit, thereby improving the throughput while maintaining tunability.

The beamline vacuum is pumped by two 220 l/s and three 60 l/s ion pumps. A differential pumping system inserted between the experimental chamber and the exit slit isolates the beamline and experiment vacuum. The experiment is mounted on a vibration isolated granite block at 26 m from the source.

4. Construction of the interferometer

The intensity interferometer, which was described previously [9], is shown schematically in fig. 4. An array of twelve slit pairs, 50 μm wide by 2 mm long with spacings ranging from 100 μm to 4 mm, selects two thin slices of the incoming x-ray beam. The slits are aligned with the aid of two Burleigh UHV inchworm motors: vertical motion is required for alignment to the x-ray

beam; horizontal motion is used to choose a pair of slits with a desired slit spacing. A small aperture in front of the slits masks off the other slit pairs. A polished quartz prism coated with gold directs the beams selected by the slits to two fast x-ray detectors. The slender prism is 5 mm wide, 48 mm high, and subtends 3° to the incident beam. A rigid frame mounted to a 20-cm diameter flange supports the entire assembly. The instrument is housed in a 40-cm-long chamber and maintained at UHV by a 45 l/s ion pump. All electrical connections to the internal components pass through feedthroughs in the main flange. The detector outputs are amplified immediately outside vacuum then pass to a correlator circuit.

To minimize the experimental measurement time for a given signal-to-noise ratio, it is important for the detectors and correlator to have as wide a bandwidth as possible, up to the reciprocal of the electron bunch time (350 ps at the NSLS). We use detectors based on microchannel plates (MCPs) because they are among the fastest x-ray detectors available. Moreover, MCPs can be operated in a linear "current" mode, which is necessary for the operation of the interferometer with the available coherent flux [9]. To attain the necessary speed, care must be taken to eliminate signal reflections due to impedance mismatch at the electron collection anodes. The detectors utilize anodes consising of two concentric cones with inner and outer half-angles of $\alpha_1 = 11°$ and $\alpha_2 = 25°$. The anode impedance is governed [10] by

$$Z = \frac{377}{2\pi} \ln\left(\frac{\tan(\alpha_2/2)}{\tan(\alpha_1/2)}\right) \quad , \tag{3}$$

giving $Z \approx 50\ \Omega$. The precision machined coaxial structures provide a good ($\pm 1\ \Omega$) impedance match between the anode and the signal preamplifier.

We measured the time response of the detectors using both a low resistance gold plated MCP and a standard inconel plated MCP. The tests were performed at the X1A beamline using 1.5-3.0 nm x-rays with the synchrotron operated in single bunch mode. The amplifier electronics consisted of two 2.2 GHz Philips 774 amplifiers and a 1.1 GHz Hewlett-Packard 54710A sampling oscilloscope. Fig. 5 shows typical detector output pulses at various bias voltages. Fitting them to a Gaussian function gives a 10 - 90% risetime of approximately 0.7 ns; the measured FWHM pulse width is $t_{meas} \approx 1.1$ ns. By correcting for the synchrotron radiation pulse width $t_{SR} \approx 0.4$ ns FWHM and time response $t_{elec} \approx 1.0$ ns of the amplifier chain, the detector response time t_{MCP} can be estimated according to

$$t_{meas}^2 = t_{elec}^2 + t_{SR}^2 + t_{MCP}^2 \quad . \tag{4}$$

It is clear that the measured response is limited by the electronics, not the detectors. To the

degree to which we could measure it, the speed of the gold and inconel plated MCPs was similar.

Measurements of the MCP output current versus the incident x-ray flux showed good linearity at 200-1000 V bias voltages, as shown in fig. 6. The incident photon flux was varied by aperturing the beam while keeping the wavelength fixed at 2.2 nm, and was monitored with an aluminum vacuum photodiode (Minuteman 423).

In parallel with detector development, we are testing a correlator circuit [9] based on a commercial double-balanced mixer and the amplifiers used in the timing measurements. Initial tests indicate that the time resolution of the prototype correlator approaches 0.5 ns. The greatest challenge we anticipate will be to reduce or eliminate sources of noise and drift in the actual experiment.

4. Conclusion

We have nearly completed construction of the interferometer and obtained satisfactory results in tests of the beam-splitting prism and detector system using the X1A soft x-ray undulator beamline. Design of the X13A beamline is complete and we are now assembling the beamline. In the future, we anticipate that the interferometer can be conveniently mounted on other undulator based beamlines. When x-ray intensity interferometry is fully developed, it is potentially applicable to the characterization of high brightness x-ray sources such as those planned for the Advanced Photon Source and the Advanced Light Source.

Acknowledgements

We would like to thank M.R. Howells for many illuminating discussions. This work was supported by the U.S. Department of Energy, Office of Basic Energy Sciences, Division of Material Sciences, under contract W-31-109-ENG-38.

References

[1] G.K. Shenoy, P.J. Viccaro, and D.M. Mills, *Characteristics of the 7-GeV Advanced Photon Source: A Guide for Users* (Argonne National Laboratory Report **ANL-88-9**, 1988).

[2] E.V. Shuryak, *Sov. Phys. JETP* **40**, 30 (1975).

[3] R. Hanbury Brown and R.Q. Twiss, *Nature* **177**, 27 (1956);
R. Hanbury Brown and R.Q. Twiss, *Nature* **178**, 1046 (1956).

[4] U. Bonse and M. Hart, *Appl. Phys. Lett.* **6**, 155 (1965).

[5] K.A. Nugent and J.E. Trebes, *Rev. Sci. Instrum.* **63**, 2146 (1992).

[6] J.W. Goodman, *Statistical Optics* , (Wiley, New York, 1985), pp. 481-510.

[7] M. Born and E. Wolf, *Principles of Optics*, (Pergamon, Oxford, 1980).

[8] H. Rarback, C. Jacobsen, J. Kirz, and I. McNulty, *Nucl. Instr. Meth.* **A266**, 96 (1988).

[9] E. Gluskin, I. McNulty, M.R. Howells, and P.J. Viccaro, *Nucl. Instr. Meth.* **319**, 213 (1992).

[10] I.A.D. Lewis and F.H. Wells, *Millimicrosecond Pulse Techniques* , (Pergamon, London, 1956) p. 288.

Figure Captions

Fig. 1. Degeneracy parameters for several undulator, wiggler and bending magnet sources at various U.S. synchrotron radiation facilities. The numbers following the source names in the legend indicate the undulator or wiggler magnetic period in centimeters. NSLS U8.0 represents the undulator at the X1 beamline at the NSLS.

Fig. 2. X13A beamline layout. The distance from the undulator to the experiment is 26 m.

Fig. 3. Calculated resolving power of the X13A SGM for various entrance/exit slit sizes (in microns). The calculation includes all aberrations but not grating figure errors.

Fig. 4. Schematic diagram of the intensity interferometer.

Fig. 5. MCP detector output pulses at various bias voltages. The incident photon wavelength was 2.2 nm.

Fig. 6. MCP detector output current vs. photon flux (as measured by Al_2O_3 vacuum photodiode) at three bias voltages ($\lambda = 2.2$ nm).

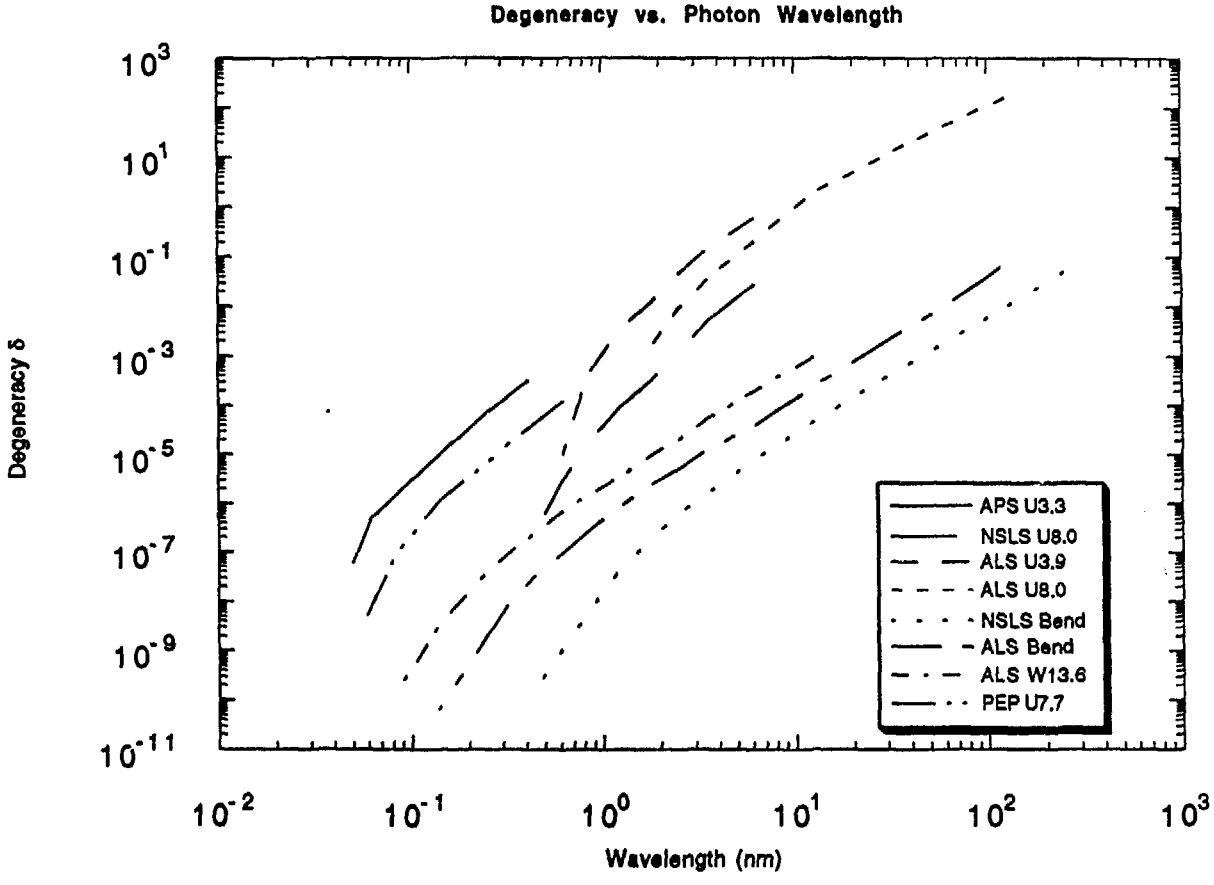
Degeneracy vs. Photon Wavelength
Degeneracy δ
10^{3}
10^{1}
10^{-1}
10^{-3}
10^{-5}
10^{-7}
10^{-9}
10^{-11}
10^{-2}
10^{-1}
10^{0}
10^{1}
10^{2}
10^{3}
Wavelength (nm)
APS U3.3
NSLS U8.0
ALS U3.9
ALS U8.0
NSLS Bend
ALS Bend
ALS W13.6
PEP U7.7

Fig. 2

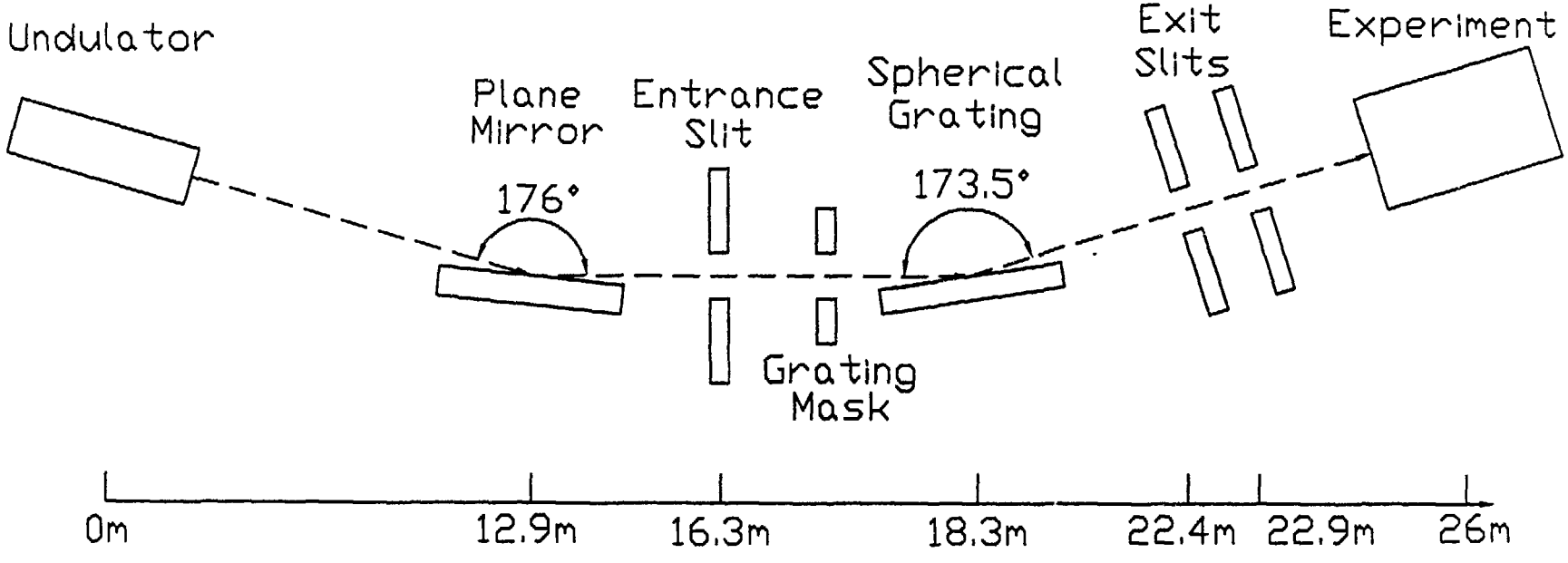
Undulator
Plane Mirror
176°
Entrance Slit
Grating Mask
Spherical Grating
173.5°
Exit Slits
Experiment
0m
12.9m
16.3m
18.3m
22.4m
22.9m
26m

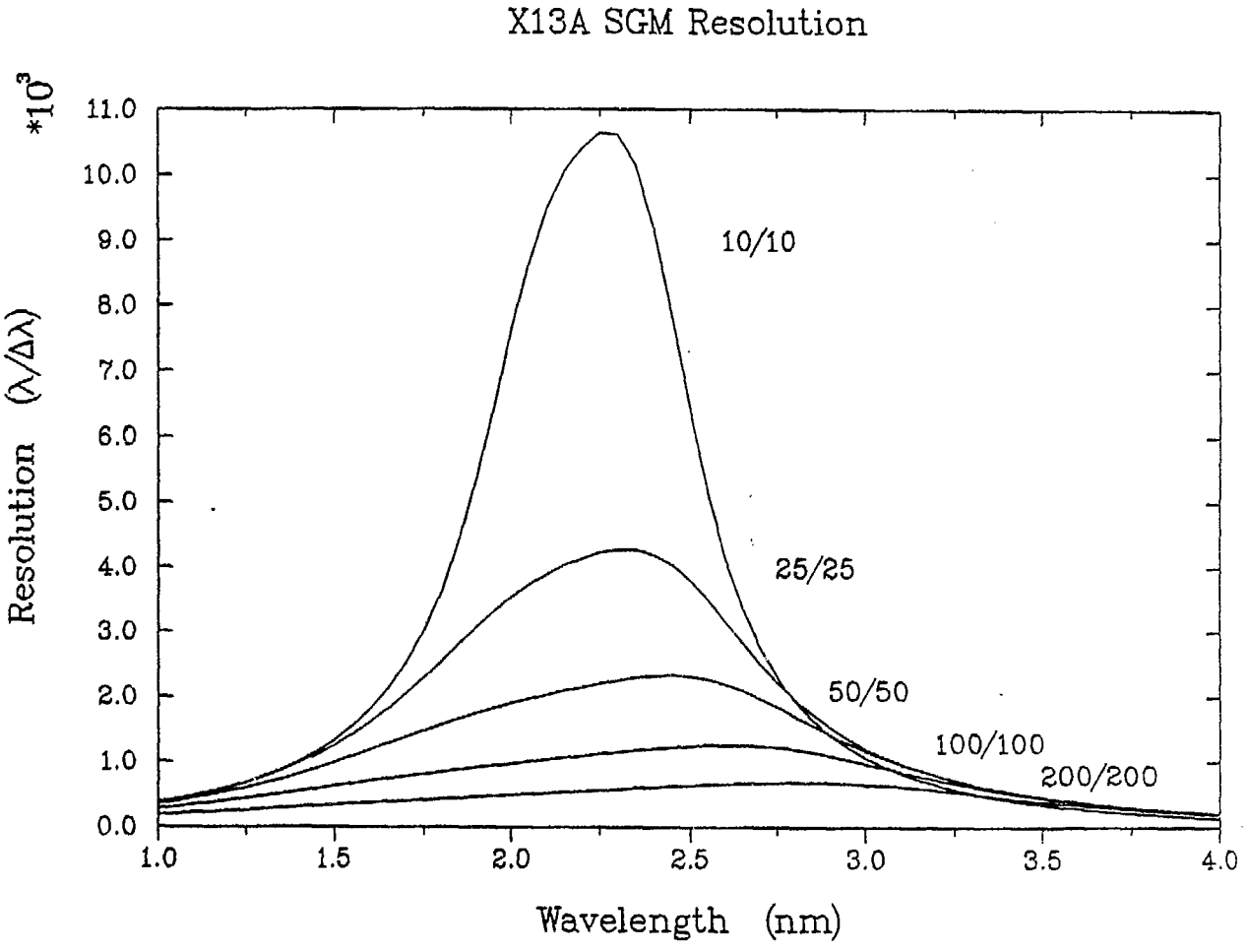
X13A SGM Resolution
Resolution (λ/Δλ)
*10^3
11.0
10.0
9.0
8.0
7.0
6.0
5.0
4.0
3.0
2.0
1.0
0.0
1.0
1.5
2.0
2.5
3.0
3.5
4.0
Wavelength (nm)
10/10
25/25
50/50
100/100
200/200

fig. 3

fig. 4

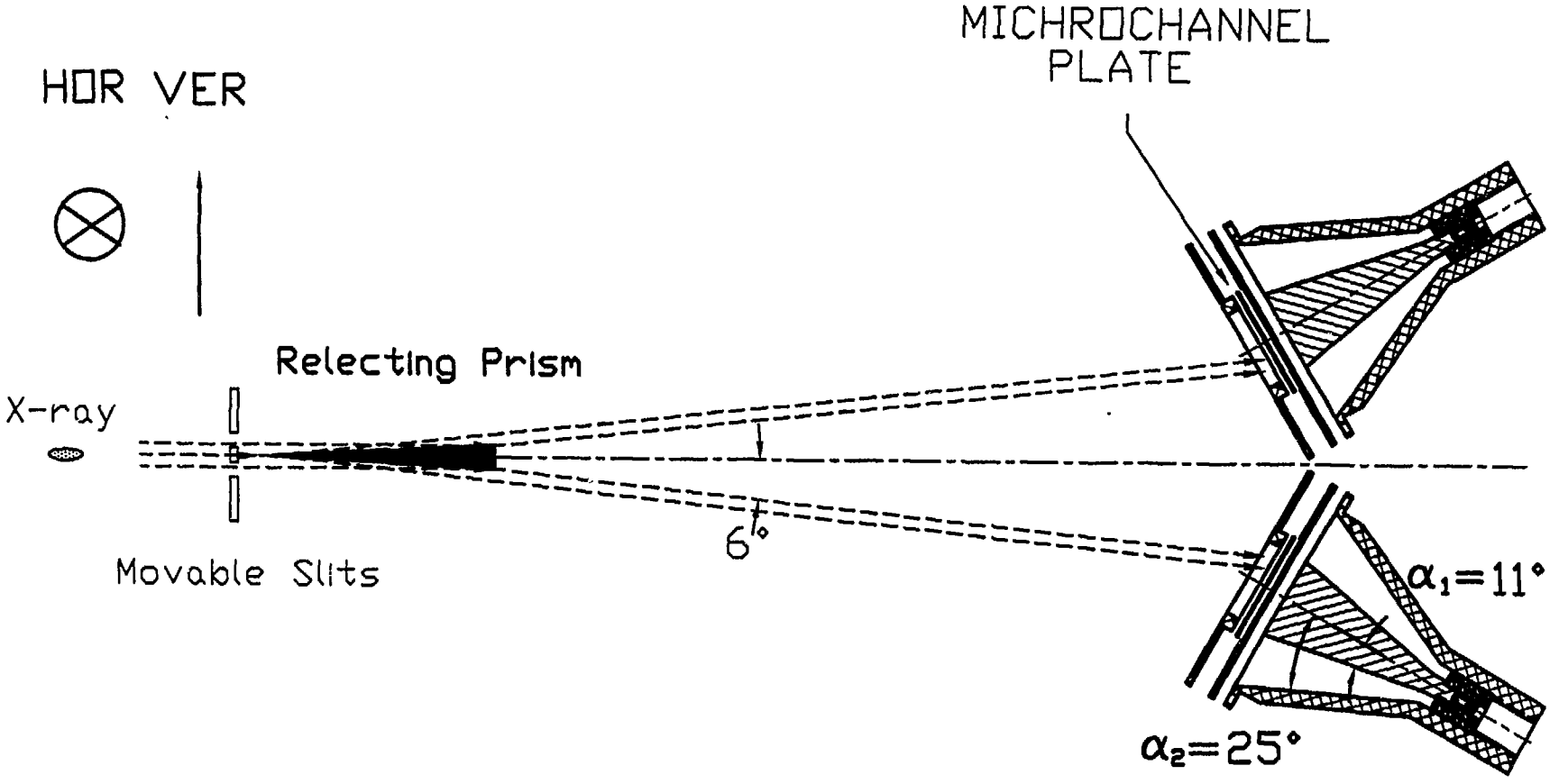
MICHROCHANNEL
PLATE
HOR VER
Relecting Prism
X-ray
6°
Movable Slits
$\alpha_1=11°$
$\alpha_2=25°$

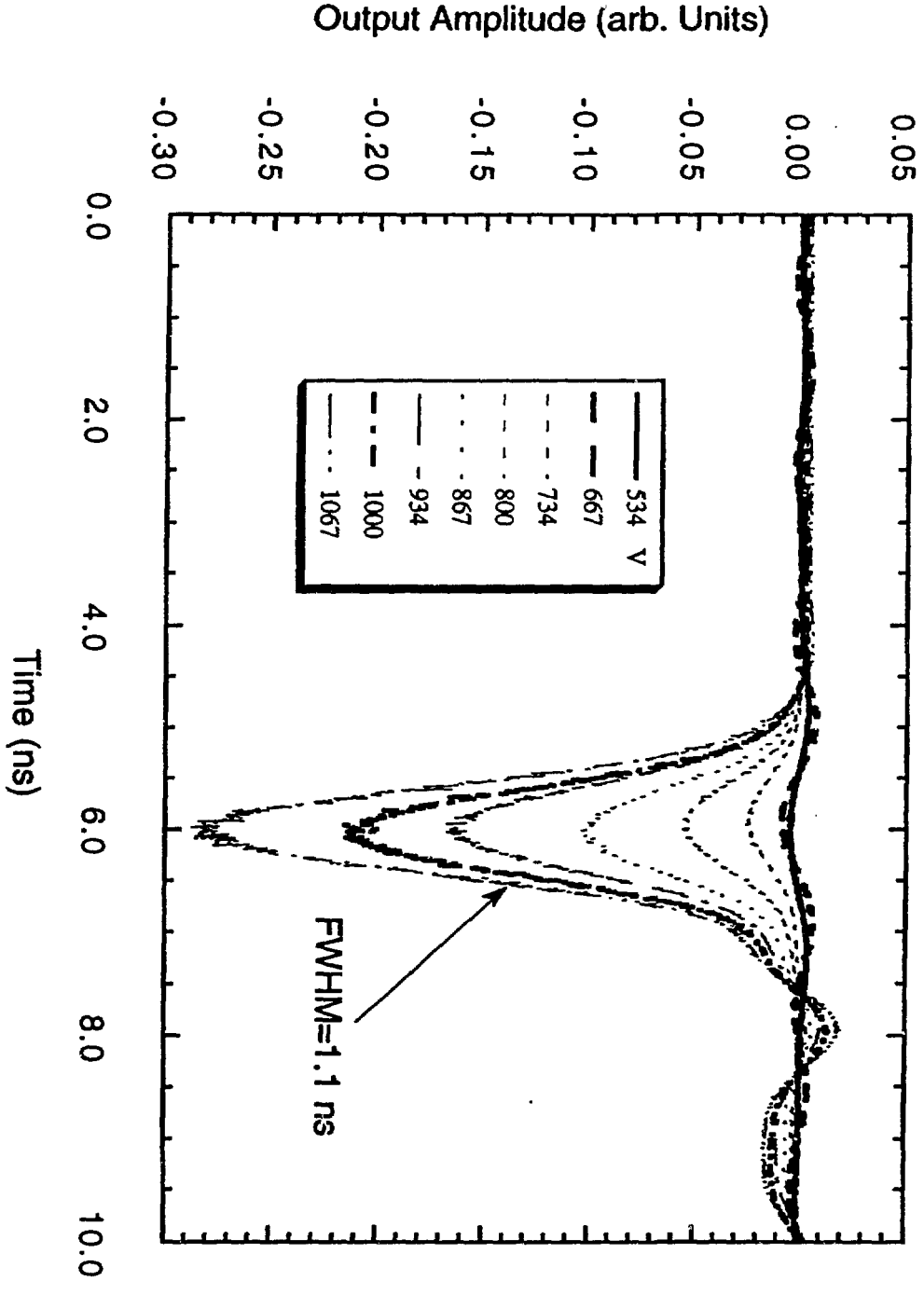
Output Amplitude (arb. Units)
0.05
0.00
-0.05
-0.10
-0.15
-0.20
-0.25
-0.30
0.0
2.0
4.0
6.0
8.0
10.0
Time (ns)
534 V
667
734
800
867
934
1000
1067
FWHM=1.1 ns

fig. 5

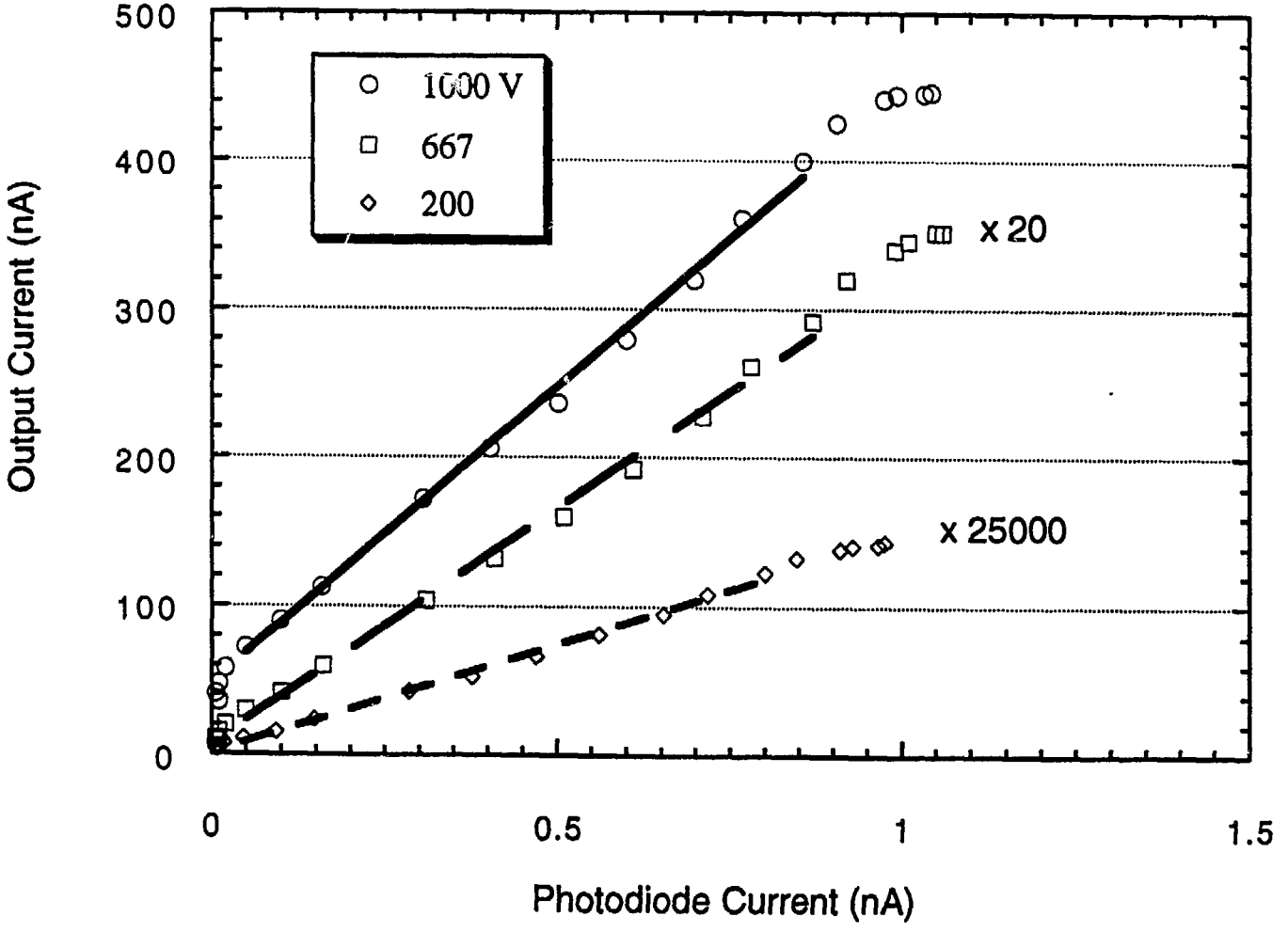
500
400
300
200
100
0
Output Current (nA)
1000 V
667
200
x 20
x 25000
0
0.5
1
1.5
Photodiode Current (nA)

Fig. 6